

ChemComm

Accepted Manuscript



This is an *Accepted Manuscript*, which has been through the Royal Society of Chemistry peer review process and has been accepted for publication.

Accepted Manuscripts are published online shortly after acceptance, before technical editing, formatting and proof reading. Using this free service, authors can make their results available to the community, in citable form, before we publish the edited article. We will replace this *Accepted Manuscript* with the edited and formatted *Advance Article* as soon as it is available.

You can find more information about *Accepted Manuscripts* in the [Information for Authors](#).

Please note that technical editing may introduce minor changes to the text and/or graphics, which may alter content. The journal's standard [Terms & Conditions](#) and the [Ethical guidelines](#) still apply. In no event shall the Royal Society of Chemistry be held responsible for any errors or omissions in this *Accepted Manuscript* or any consequences arising from the use of any information it contains.

COMMUNICATION

3D Networked Polydiacetylene Sensor for Enhanced Sensitivity

Cite this: DOI: 10.1039/x0xx00000x

Subum Lee^a, Joosub Lee^b, Dong Wook Lee^a, Jong-Man Kim^{*b,c} and Haiwon Lee^{*a,c}

Received 00th October 2015,
Accepted 00th January 2015

DOI: 10.1039/x0xx00000x

www.rsc.org/

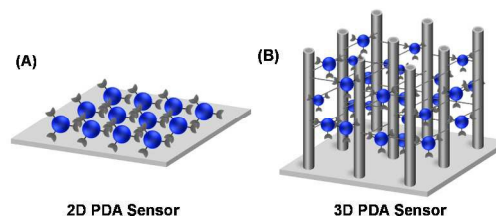
A three order of sensitivity enhancement over a 2D system was achieved with a polydiacetylene-immobilized 3D networked sensor matrix.

Since the first report of a polydiacetylene (PDA)-based colorimetric influenza-virus sensor,¹ the structurally unique conjugated polymer has been actively investigated as a key component in a variety of sensor formats.²⁻²⁹ PDAs are intrinsically supramolecular aggregates because they are prepared from polymerization (UV light, γ -ray irradiation or heat) of self-assembled diacetylene (DA) aggregates.³⁰⁻³⁶ A hand-held laboratory 254 nm UV lamp, in general, can effectively induce polymerization of self-assembled DA aggregates. Accordingly, preparation of PDAs is relatively easy compared to common conjugated polymers which are chemically synthesized. The densely packed nature of the polymer restricts conformational mobility of main chain backbones and enables extensive and efficient p-orbital overlap. As a result, PDAs generally have an absorption maximum at around 650 nm that corresponds to a blue color. When the aggregated, blue colored supramolecular PDAs are exposed to various physical (mechanical strain, temperature, etc) and chemical/biochemical (pH, solvent, specific ligand-receptor interactions, etc) inputs, the polymers undergo a blue-to-red color transition and the absorption maximum shifts to around 550 nm.

In addition to the brilliant blue-to-red color transition, PDAs display a unique 'turn-on' fluorescence feature upon environmental stimulation. The stimulus-induced 'turn-on' fluorescence has allowed fabrication of various label-free PDA-based sensor chips.³⁷⁻⁴⁶ In general, the PDA sensor chips are prepared by immobilization of blue-phase, non-fluorescent PDA particles on the solid substrates. Red fluorescence signals are monitored when the PDA chip is exposed to the targeted stimulus. The majority of PDA-based sensor chips, however, have been formatted as two dimensional (2D) structures and this has created an intrinsic limitation associated with the sensitivity of the PDA sensor chip. For instance, in our previous report that describes the first PDA based microarrayed sensor chip, the detection limit of the sensor chip

was in the range of millimolar concentration when a PDA-cyclodextrin interaction was used as a model system.⁴⁶ To overcome the intrinsic limitations associated with the 2D format, we have developed a 3D networked PDA sensor system. Herein, we demonstrate that immobilization of PDA vesicles on 3D networked nanostructures affords a significant increase in the sensitivity of the polymer. A three order of sensitivity enhancement over a 2D system was observed with the 3D networked sensor matrix. As depicted in Scheme 1, The increased numbers of immobilized PDA vesicles and large free volumes that exist in the 3D sensor matrix are the key to the enhanced sensitivity.

In order to fabricate the 3D networked PDA sensor system, micropillar structures were prepared on a p-type silicon (100) substrate by a silicon deep etching process (Fig. 1, B).⁴⁷⁻⁴⁸ The diameter, height, and the inter-pillar gap were 1 μm , 5 μm , and 4 μm respectively. We have found that if the interpillar distance is too short (< 1 μm), immobilization of PDA vesicles was not efficient due to the PDA particle size (ca. 100-300 nm). Networked carbon nanotubes (CNTs) were fabricated using the procedures reported in our group (Fig. 1, C).⁴⁷ To enhance the mechanical strength and to introduce amine functional groups, the 3D CNT networked pillared structures were coated with Al_2O_3 (thickness: 5 nm) using an atomic layer deposition (ALD) method (Fig. 1, D). The Al_2O_3 coated 3D networked substrate was treated with a 3-aminopropylmethyl-diethoxysilane (APMDES) solution (toluene, 1 h) to yield surface amine moieties. For comparison, a silicon wafer



Scheme 1 Schematic representation of 2D (A) and 3D (B) PDA sensors.

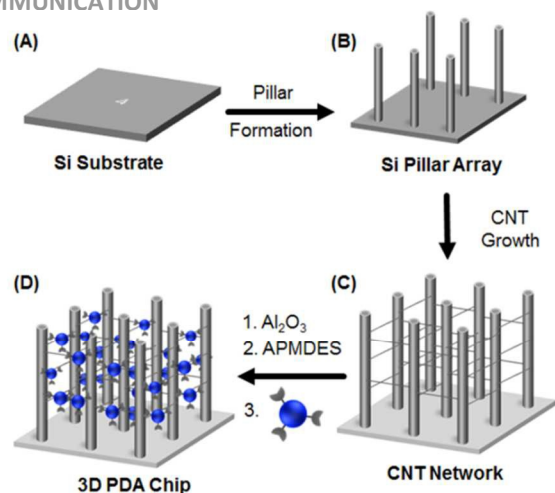


Fig. 1 Schematic for the fabrication of a 3D networked PDA sensor.

with no pillared structures was also treated with an APMDDES solution for a 2D sensor chip. Diacetylene vesicles were prepared from 9:1 mixtures of 10,12-pentacosadiynoic acid (PCDA) and its *n*-hydroxysuccinimide form (PCDA-NHS) by employing a standard vesicle forming process to form an aqueous 1 mM diacetylene suspension.⁴⁹ The amine modified 2D and 3D networked chips were incubated in a diacetylene suspension (diluted to 0.25 mM) for 30 min at ambient temperature with stirring at 800 rpm. The diacetylene immobilized sensor chips were washed with deionized water and were irradiated with 254 nm UV light (1 mW/cm²) for 2 min to induce photopolymerization. It should be noted that 3D networked PDA chip can be also achieved by immobilization of photopolymerized diacetylene vesicles.

Fig. 2A and 2B display SEM images of CNT-networked pillar structures.

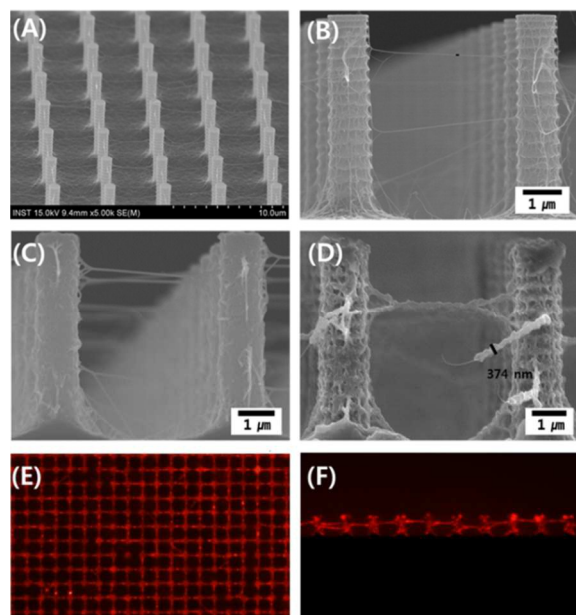


Fig. 2 (A-D) SEM images of networked CNT (A,B), after Al₂O₃ deposition (C), and after immobilization of PDA vesicles (D). Fluorescence microscopic images of the PDA immobilized networked structures from top (E) and side (F) views.

The thickness of the CNT was found to be ca. 27 nm. Fig. 2C shows a SEM image of the CNT networked pillar structure after

deposition of Al₂O₃ (thickness: ca 5 nm). The SEM image presented in Fig. 3D shows that PDAs are coated on the pillars and interconnected Al₂O₃ coated CNT networks. In order to prove that PDAs are immobilized on the surface of the 3D structures, fluorescent microscopic images of the PDA-treated samples were obtained (Figs. 2E and 2F). The fluorescence image of top view of the 3D structure clearly indicates that PDA vesicles are effectively immobilized (Fig. 2E). In addition, the fluorescence microscopic image taken from the side view of the sample further proves the efficiency of the PDA immobilization. It should be noted that the images shown in Fig. 2E and 2F are obtained after heat treatment (100 °C, 1 min) of the PDA immobilized sensor chip to induce a blue-to-red transition of the PDA since PDAs in the blue phase are non-fluorescent.

Previously, we reported that cyclodextrins (CDs) can disrupt the ordered structures of PDA supramolecules and form inclusion complexes with PDAs (Fig. 3A).⁵⁰ The mechanical strain energy generated in the formation of inclusion complexes between CD molecules and PDA supramolecules is transferred to the conjugated ene-yne backbone of the polymer. This causes partial distortion of the polymer backbone and reduces effective overlap of the conjugated p-orbitals, resulting in the blue-to-red color transition. We also found that α -CD is superior to β - and γ -CDs in terms of the capability of the colorimetric transition. Thus, the CD-PDA interaction can serve as a good model for the enhanced sensitivity test for the 3D networked PDA sensor system.

In order to compare the efficiency of the PDA sensors, the conjugated polymer-immobilized chips in a 2D and 3D format were exposed to α -CD solution of various concentrations. The 2D PDA sensor chip was prepared by immobilizing PDA vesicles on an amine modified silicon wafers under a similar condition used for the 3D sensor. As displayed in Fig. 3B, fluorescence signals from 2D PDA sensors were hardly observable until 2.5 mM of α -CD. In contrast, a

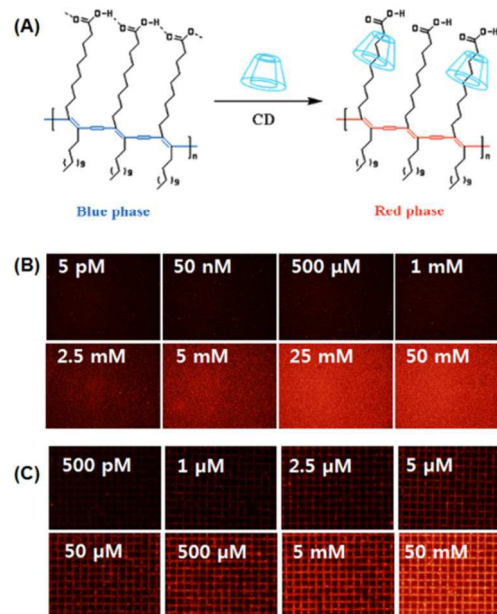


Fig. 3 (A) Schematic of a PDA-cyclodextrin interaction. (B-C) Fluorescence microscopic images 2D (B) and 3D (C) PDA sensors obtained after exposure to various concentrations of α -CD.

red fluorescence from the PDA was monitored upon incubation of a 3D networked PDA chip in a α -CD solution of 2.5 μ M (Fig. 3C). This observation clearly demonstrates that a 3D networked PDA sensor chip displays a higher sensitivity over a 2D immobilized PDA sensor.

Because it is difficult to measure the surface area of the 3D networked sensor system directly, we calculated the theoretical surface area of the 3D networked sensor platform and compared it to that of the 2D sensor platform. The calculated surface area of pillared CNT networked 3D sensor platform (dimension: 1 mm x 1 mm, pillar gap: 4 μ m, pillar diameter: 1 μ m, pillar height: 5 μ m) is approximately 2.0×10^{-6} m² while that of 2D platform is 1.0×10^{-6} m². Thus the surface area for 3D sensor system is approximately two fold larger than that of the 2D sensor. Thus, the increase in the surface area is not significantly large in light of the high sensitivity of the 3D sensor system. The large increase in the sensitivity for 3D sensor system is presumably a consequence of the significant increase in the accessibility of cyclodextrin molecules that interact with PDAs through the large free volume exist in the sensor matrix

Fig. 4 displays plots of fluorescence intensity as a function of α -CD concentration. The fluorescence intensity of a 2D PDA sensor chip remained unchanged until it is exposed to millimolar concentrations of α -CD and displays a sharp increase at 2.5 mM of CD. In contrast, the fluorescence intensity of the CD-exposed 3D networked PDA sensor chip increases gradually from micromolar to millimolar CD concentration. The different behavior in the fluorescence intensity between the two different sensor formats is presumably due to the different accessibility of CD molecules. The aggregated nature of the PDA vesicles on the 2D chip prevents facile access of the CD molecules and the sensor system requires a high concentration of CD for efficient CD-PDA interaction. In the case of 3D networked PDA sensor system, CD molecules can interact freely with the conjugated polymers and generates fluorescence signals from low concentration of the CD. The detection limit of the 2D and 3D networked sensor systems was found to be 2.5 mM and 2.0 μ M, respectively. Thus, at least three order increase in the sensitivity was obtained with the 3D sensor system over the 2D format.

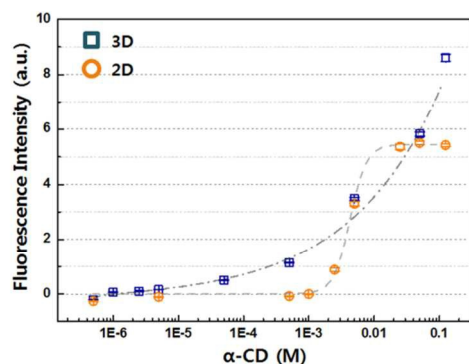


Fig. 4 Plot of fluorescence intensity of PDA sensors in 2D and 3D formats as a function of α -CD concentration (log scale)

In summary, we have developed a new 3D PDA sensor system. Immobilization of PDA vesicles on the surface of the modified CNT-

networked pillared structures afforded a 3D networked sensor system. More than three order increase in the sensitivity was observed with the 3D networked sensor matrix in comparison with a conventional 2D PDA sensor system. Although the current study focuses on the molecular recognition event between PDA and cyclodextrin, the strategy described above can be utilized for the detection of chemically and biochemically interesting target molecules including DNAs, proteins, ions and surfactants with enhanced sensitivity. Furthermore, the 3D networked sensor platform should not be restricted to the PDA sensor system. Other probe molecules could be potentially immobilized to the surface of the 3D networked for the construction of signal amplified sensor systems

The authors thank the National Research Foundation of Korea for financial support (2012M3A7B4035286, 2014R1A2A1A01005862, 2012R1A6A1029029).

Notes and references

^a Department of Chemistry, Hanyang University, Seoul 133-791, Korea. E-mail: haiwon@hanyang.ac.kr

^b Department of Chemical Engineering, Hanyang University, Seoul 133-791, Korea. E-mail: jmk@hanyang.ac.kr

^c Institute of Nano Science and Technology, Hanyang University, Seoul 133-791, Korea.

- D. H. Charych, J. O. Nagy, W. Spevak, M. Bednarski, *Science*, 1993, **261**, 585.
- X. Sun, T. Chen, S. Huang, L. Lia, H. Peng, *Chem. Soc. Rev.*, 2010, **39**, 4244.
- O. Yarimaga, J. Jaworski, B. Yoon, J.-M. Kim, *Chem. Commun.*, 2012, **48**, 2469.
- X. Chen, G. Zhou, X. Peng, J. Yoon, *Chem. Soc. Rev.*, 2012, **41**, 4610.
- H. Jiang, R. Jelinek, *Langmuir*, 2015, **31**, 5843.
- K. P. Kootery, H. Jiang, S. Kolusheva, T. P. Vinod, M. Ritenberg, L. Zeiri, R. Volinsky, D. Malferrari, P. Galletti, E. Tagliavini, R. Jelinek, *ACS Appl. Mater. Interfaces*, 2014, **6**, 8613.
- J. Lee, H. T. Chang, H. An, S. Ahn, J. Shim, J. -M. Kim, *Nat. Commun.*, 2013, **4**, 2461.
- J. Lee, M. Pyo, S. -h. Lee, J. Kim, M. Ra, W. -Y. Kim, B. J. Park, C. W. Lee, J. -M. Kim, *Nat. Commun.*, 2014, **5**, 3736.
- D.-H. Park, J. Hong, I. S. Park, C. W. Lee, J.-M. Kim, *Adv. Funct. Mater.*, 2014, **24**, 5186.
- S. Lee, J. Lee, M. Lee, Y. K. Cho, J. Baek, J. Kim, S. Park, M. H. Kim, R. Chang, J. Yoon, *Adv. Funct. Mater.*, 2014, **24**, 3699.
- X. Wang, X. Sun, P. A. Hu, J. Zhang, L. Wang, W. Feng, S. Lei, B. Yang, W. Cao, *Adv. Funct. Mater.*, 2013, **23**, 6044.
- S. Seo, J. Lee, M. S. Kwon, D. Seo, J. Kim, *ACS Appl. Mater. Interfaces*, 2015, **7**, 20342.
- X. Chen, L. Li, X. Sun, Y. Liu, B. Luo, C. Wang, Y. Bao, H. Xu, H. Peng, *Angew. Chem. Int. Ed.*, 2011, **50**, 5486.
- H. Jiang, Y. Wang, Q. Ye, G. Zou, W. Su, Q. Zhang, *Sens. Actuators: B.*, 2010, **143**, 789.
- T. Eaidkong, R. Mungkarndee, C. Phollookin, G. Tumcharern, M. suk wattanasinitt, S. Wacharasindhu, *J. Mater. Chem.*, 2012, **22**, 5970.
- B. W. Davis, A. J. Burris, N. Niamnont, C. D. Hare, C. -Y. Chen, M. Suk wattanasinitt, Q. Cheng, *Langmuir*, 2014, **30**, 9616.

17. Q. Cheng, R. C. Stevens, *Langmuir*, 1998, **14**, 1974.
18. H. Jeon, J. Lee, M. H. Kim, J. Yoon, *Macromol. Rapid. Commun.*, 2012, **33**, 972.
19. J. Lee, E. J. Jeong, J. Kim, *Chem. Commun.*, 2011, **47**, 358.
20. J. Lee, S. Seo, J. Kim, *Adv. Funct. Mater.*, 2012, **22**, 1632.
21. G. Yang, W. Hu, H. Xia, G. Zou, Q. Zhang, *J. Mater. Chem. A.*, 2014, **2**, 15560.
22. Y. Li, L. Wang, X. Yin, B. Ding, G. Sun, T. Ke, J. Chen, J. Yu, *J. Mater. Chem. A.*, 2014, **2**, 18304.
23. R. Pimsen, A. Khumsri, S. Wacharasindhu, G. Tumcharern, M. Sukwattanasinit, *Biosens. Bioelectron.*, 2014, **62**, 8.
24. S. Lu, F. Luo, X. Duan, C. Jia, Y. Han, H. Huang, *J. Appl. Polym. Sci.* 2014, **131**, 40634.
25. Y. Xu, J. Le, W. Hu, G. Zou, Q. Zhang, *J. Colloid Interface Sci.*, 2013, **400**, 116.
26. R. A. Nallicheri, M. F. Rubner, *Macromolecules*, 1991, **24**, 517.
27. P. Samyn, J. R uhe, M. Biesalski, *Langmuir*, 2010, **26**, 8573.
28. K. M. Kim, D. J. Oh and K. H. Ahn, *Chem. Asian J.*, 2011, **6**, 122.
29. J. Jaworski, K. Yokoyama, C. Zueger, W.-J. Chung, S.-W. Lee and A. Majumdar, *Langmuir*, 2011, **27**, 3180.
30. G. Wegner, *Z. Naturforsch.*, 1969, **24**, 824.
31. J. W. Lauher, F. W. Fowler and N. S. Goroff, *Acc. Chem. Res.*, 2008, **41**, 1215.
32. J. R. N abo, S. Rondeau-Gagn e, C. Vigier-Carri re, J.-F. Morin, *Langmuir*, 2013, **29**, 3446.
33. T.-J. Hsu, F. W. Fowler, J. W. Lauher, *J. Am. Chem. Soc.*, 2012, **134**, 142.
34. S. B. Lee, R. Koepsel, D. B. Stolz, H. E. Warriner and A. J. Russell, *J. Am. Chem. Soc.*, 2004, **126**, 13400.
35. Y. Lu, Y. Yang, A. Sellinger, M. Lu, J. Huang, H. Fan, R. Haddad, G. Lopez, A. R. Burns, D. Y. Sasaki, J. Shelnett and C. J. Brinker, *Nature*, 2001, **410**, 913.
36. Y. Lifshitz, Y. Golan, O. Konovalov, A. Berman, *Langmuir*, 2009, **25**, 4469.
37. D. J. Ahn, J.-M. Kim, *Acc. Chem. Res.*, 2008, **41**, 805.
38. J. U. Lee, J. H. Jeong, D. S. Lee, S. J. Sim, *Biosens. Bioelectron.*, 2014, **61**, 314.
40. S. H. Won, S. J. Sim, *Analyst*, 2012, **137**, 1241.
41. I. K. Kwon, M. S. Song, S. H. Won, S. P. Choi, M. Kim, S. J. Sim, *Small*, 2012, **8**, 209.
42. S. Seo, J. Lee, E.-J. Choi, E.-J. Kim, J.-Y. Song, J. Kim, *Macromol. Rapid Commun.*, 2013, **34**, 743.
43. J. Lee, H.-J. Kim, J. Kim, *J. Am. Chem. Soc.*, 2008, **130**, 5010.
44. S.-H. Eo, S. Song, B. Yoon, J.-M. Kim, *Adv. Mater.*, 2008, **20**, 1690.
45. H. Jiang, Y. Wang, Q. Ye, G. Zou, W. Su., Q. Zhang, *Sensor. Actuat. B*, 2010, **143**, 789.
46. J.-M. Kim, Y. B. Lee, D. H. Yang, J.-S. Lee, G. S. Lee, D. J. Ahn, *J. Am. Chem. Soc.*, 2005, **127**, 17580.
47. J. Seo, T. Lee, S. Ko, H. Yeo, S. Kim, T. Noh, S. Song, M. Sung, H. Lee, *Adv. Mater.*, 2012, **24**, 1975.
48. J. Seo, T. J. Lee, C. Lim, S. Lee, C. Rui, D. Ahn, S. B. Lee, H. Lee, *Small*, 2015, **11**, 2990
49. J.-M. Kim, E.-K. Ji, S. M. Woo, H. Lee, D. J. Ahn, *Adv. Mater.*, 2003, **15**, 1118.
50. J.-M. Kim, J.-S. Lee, J.-S. Lee, S.-Y. Woo, D. J. Ahn, *Macromol. Chem. Phys.*, 2005, **206**, 2299.